Heliyon

Received:
2 July 2018
Revised:
31 October 2018
Accepted:
26 November 2018

Cite as: Markus Tammia, Ruifa Mi, Valentin M. Sluch, Allen Zhu, Tiffany Chung, Daniel Shinn, Donald J. Zack, Ahmet Höke, Hai-Quan Mao. Egr2 overexpression in Schwann cells increases myelination frequency *in vitro*. Heliyon 4 (2018) e00982. doi: 10.1016/j.heliyon.2018.e00982

Egr2 overexpression in Schwann cells increases myelination frequency *in vitro*

Markus Tammia [a,b,c], Ruifa Mi [d,e], Valentin M. Sluch [f], Allen Zhu [g], Tiffany Chung [a], Daniel Shinn [g], Donald J. Zack [f,h,i], Ahmet Höke [d,e], Hai-Quan Mao [a,b,c,g,*]

[a] *Institute for NanoBioTechnology, Johns Hopkins University, Baltimore, MD 21218, USA*

[b] *Department of Materials Science and Engineering, Whiting School of Engineering, Johns Hopkins University, Baltimore, MD 21218, USA*

[c] *Translational Tissue Engineering Center, Johns Hopkins University School of Medicine, Baltimore, MD 21287, USA*

[d] *Department of Neuroscience, Johns Hopkins University School of Medicine, Baltimore, MD 21205, USA*

[e] *Department of Neurology, Johns Hopkins University School of Medicine, Baltimore, MD 21205, USA*

[f] *Department of Molecular Biology and Genetics, Johns Hopkins University School of Medicine, Baltimore, MD 21205, USA*

[g] *Department of Biomedical Engineering, Johns Hopkins University School of Medicine, Baltimore, MD 21205, USA*

[h] *Department of Ophthalmology, Wilmer Eye Institute, Johns Hopkins University School of Medicine, Baltimore, MD 21287, USA*

[i] *Institute of Genetic Medicine, Johns Hopkins University School of Medicine, Baltimore, MD 21287, USA*

[*] Corresponding author.
E-mail address: hmao@jhu.edu (H.-Q. Mao).

Abstract

Schwann cells are key players in peripheral nerve regeneration, and are uniquely capable of remyelinating axons in this context. Schwann cells orchestrate this process via a set of transcription factors. While it has been shown that overexpression of specific genes, *e.g. Egr2,* upregulates myelin-related transcripts, it remains unknown if such manipulation can functionalize the cells and enhance their myelination frequency. The ability to do so could have implications in the use of human stem cell-derived Schwann cells, where myelination is hard to achieve. After screening four candidate transcription factors (*Sox10, Oct6, Brn2* and *Egr2*), we found that overexpression of *Egr2* in

https://doi.org/10.1016/j.heliyon.2018.e00982

rat Schwann cells co-cultured with sensory neurons enhanced myelination frequency and reduced cell proliferation. However, in a mouse model of sciatic nerve repair with cells engrafted within a nerve guide, myelination frequency in the engrafted cells was reduced upon *Egr2* overexpression. Our results show that while overexpression of *Egr2* can enhance the myelination frequency *in vitro*, it is context-dependent, potentially influenced by the microenvironment, timing of association with axons, expression level, species differences, or other factors.

Keywords: Neuroscience, Cell biology

1. Introduction

As the key players in peripheral nerve regeneration, Schwann cells have gained much attention for cell-based nerve regeneration therapies in both the peripheral and central nervous systems. Upon acute injury to the peripheral nervous system, Schwann cells become activated and transdifferentiate into a pro-regenerative phenotype that secrete neurotrophic factors, clear myelin debris through autophagocytosis and recruitment of macrophages, organize into guiding structures within existing channels of basal lamina to what are called bands of Büngner, and ultimately remyelinate the regenerating axons (Jessen and Mirsky, 2016). Among these activities, remyelination and trophic support for recruitment of immune cells and axon guidance are key for cell therapies. During the repair process, remyelination may be compromised, and can be especially hard to obtain at high efficiency using Schwann cells derived through lineage reprogramming (Keilhoff et al., 2006; Liu et al., 2012; Thoma et al., 2014). One possible approach to obtain highly functional, remyelinating Schwann cells is to harness the transcription factors that control the cell-intrinsic process of myelination. During myelination, *Sox10* takes part in the upregulation of *Oct6* (also known as *Pou3f1*, *Tst1* or *Scip*) (Jagalur et al., 2011), and together they act to upregulate *Egr2* (also known as *Krox20*) (Ghislain and Charnay, 2006), which regulates the expression of key myelin components (Topilko et al., 1994). Mature myelin is formed upon downregulation of *Oct6* (Monuki et al., 1990) with maintained *Sox10* (Bremer et al., 2011) and *Egr2* (Decker et al., 2006) expression. Another transcription factor called *Brn2* (or *Pou3f2*) is related to *Oct6* and can take its place and rescue myelination in *Oct6*-deficient mice (Jaegle et al., 2003; Stolt and Wegner, 2016). While it has been shown that enforced expression of *Egr2* leads to upregulation of myelin transcripts (Nagarajan et al., 2001), it has not been shown whether or not it is a feasible approach for cell functionalization in order to enhance myelination frequency, since ectopic expression may induce a detrimental endoplasmic reticulum stress response (Latasa et al., 2010). We therefore set out to determine if overexpression of the key transcription factors may enhance Schwann cell myelination frequency in an *in vitro* myelination model, and if functionalized Schwann cells may better support axonal regeneration when engrafted into an *in vivo* nerve regeneration model.

https://doi.org/10.1016/j.heliyon.2018.e00982

2. Materials and methods

2.1. Cloning, production and titration of lentiviral vectors

Gateway entry clones for human *Sox10* (NM_006941.3), *Brn2* (BC051699.1), and *Egr2* (NM_000399.2) were obtained from the Johns Hopkins University High Throughput Biology Center. Human *Oct6* (NM_002699.3) was amplified by PCR from a TrueClone cDNA vector (Origene, plasmid SC317737, Rockville, MD, USA) using Q5 High-Fidelity Polymerase with the forward primer (5′- GCG AAT TCG GCG GCA TG -3′) and reverse primer (5′- CAA TCT AGA TCA CTG CAC TGA GCC GG -3′), and cloned into pENTR1A no ccDB (w48-1), a gift from Eric Campeau (Addgene plasmid #17398, Cambridge, MA, USA), between the EcoRI and XbaI sites using the Rapid DNA Ligation Kit (Roche, Basel, Switzerland). Myc-DDK (DDK is also known as a FLAG tag) entry clones for *Egr2* were created by Gibson assembly with the PCR product from an *Egr2-Myc-DDK* containing plasmid (Origene RC212183, NM_000399.2) using forward primer (5′- CTG GAT CCG GTA CCG ATC GCC ATG ATG ACC GCC -3′) and reverse primer (5′- TCG AGT GCG GCC GCG TTA AAC CTT ATC GTC GTC ATC CTT G -3′) as insert and pENTR1A no ccDB (w48-1) digested with EcoRI-HF (NEB, Ipswich, MA, USA) as the backbone, and assembled using the Gibson Assembly Master Mix (NEB). Transfer vectors were then created through an LR clonase II reaction (Thermo Fisher Scientific, Lafayette, CO, USA) into pLenti CMV Blast DEST (706-1), a gift from Eric Campeau (Addgene plasmid # 17451). A bi-cistronic transfer vector for *Egr2* and *mCherry* using a 2A peptide was created by cloning *Egr2* from the above transfer vector by PCR using forward primer (5′- TAT ATC TAG AAT GAT GAC CGC CAA GGC CGT AG -3′) and reverse primer (5′- TAT AGG ATC CCT ATC AAG GTG TCC GGG TCC GAG -3′), and ligating between the XbaI and BamHI sites of pUltra-hot, a gift from Malcolm Moore (Addgene plasmid #24130). A GFP with a nuclear localization signal (nuclear GFP) in the pLenti-CMV Blast DEST backbone was a gift from Donald Zack. All constructs had the CDS and insertion sites verified by Sanger DNA sequencing (Genewiz, South Plainfield, NJ, USA), and were expanded in Stbl3 cell hosts (Thermo Fisher).

For lentivirus production, HEK 293T cells, a gift from Donald Zack, were plated at 4 million live cells per plate in 8 ml of DMEM/F12 supplemented with 10% HI-FBS, 1x MEM non-essential amino acid solution, 1 mM sodium puryvate, penicillin (100 U/ml) and streptomycin (100 μg/ml, all from Thermo Fisher), onto poly-(D)-lysine-coated 10 cm dishes (Sigma-Aldrich, St. Louis, MI, USA). The next day, 15 μg/plate of the VSV-G envelope plasmid pMD2.g (Addgene plasmid #12259), 6 μg/plate of pMDLg/pRRE (Addgene plasmid #12251), 6 μg/plate pRSV-Rev (Addgene plasmid #12253), all gifts from Didier Trono, as well as 15 μg/plate of respective transfer vector was combined to a final plasmid concentration of 100 μg/ml. Then, linear poly(ethyleneimine) (Polymer Chemistry Innovations, Inc., Vista,

https://doi.org/10.1016/j.heliyon.2018.e00982

CA, USA) was added to the mixture at nitrogen to phosphate molar ratio of 6, and the polyplexes added to the cells for 4 hours before the media was exchanged. The following day, 10 mM sodium butyrate (Sigma-Aldrich) was added to the media. Two days after transfection, the supernatant was collected and viruses concentrated using Lenti-X concentrator (Clonetech, Palo Alto, CA, USA) according to the manufacturer's instructions, aliquots prepared in PBS and stored at −80 °C.

To determine the multiplicity of infection (MOI), purified primary rat Schwann cells were infected with a serial 1:10 dilution of the nuclear GFP lentivirus in the presence of 8 μg/ml of polybrene (Sigma-Aldrich) over night, then detached four days after transduction using TrypLE Express (Thermo Fisher) and fixed with 1% paraformaldehyde in PBS before analyzing transduction efficiency by flow cytometry. Cells were considered positive when their expression level was above 99.9% of the cells in a non-transduced control sample. MOI was calculated for samples with 2−20% transduction efficiency. After this, titration was performed using a PCR kit (Applied Biological Materials, Richmond, BC, Canada) on all other constructs and batches of lentiviruses, and their MOI determined by their relative viral titer to the nuclear GFP vector.

2.2. Cell isolation and purification

Primary rat Schwann cells were isolated from Sprague Dawley rat postnatal day 4 pups using the methods described by Brockes (Brockes et al., 1979) with slight modifications. Briefly, sciatic nerves were dissected and epineurium removed. The nerves were then digested with collagenase type I (Thermo Fisher) at 3 mg/ml in L-15 medium for 45 minutes at 37 °C, further treated with 0.375 mg/ml DNase (Thermo Fisher) and 0.0625% Trypsin EDTA (Thermo Fisher, diluted from 0.25% solution) for 15 min at 37 °C. The reaction was stopped by addition of DMEM containing 10% HI-FBS, nerves washed with L-15, and then triturated to release the cells and plated onto TCPS coated with collagen (Nutragen, 1:30 dilution, Advanced BioMatrix, Poway, CA, USA) in DMEM with high glucose, no sodium puryvate (Thermo Fisher), 10 μg/ml of piperacillin and ciprofloxacin (Sigma-Aldrich) and 10% HI-FBS (Thermo Fisher) (media composition hereafter referred to as D10). The day after plating, Ara-c was added to the media at 10 μM for 2−3 days, after which cells were cultured in D10 with 200 μg/ml of bovine pituitary extract and 2 μM forskolin (both from Sigma-Aldrich). Cells were passaged by detaching with Accutase (Sigma-Aldrich), incubated with anti-Thy1 from hybridoma supernatant at a 1:100 dilution (TIB-103, American Type Culture Collection, Manassas, VA, USA) for 30 minutes at 37 °C, washed with DMEM and incubated with rabbit complement diluted 1:8 (MP Biomedicals, Aurora, OH, USA), before plating at a 1:2−1:3 seeding ratio. Media was exchanged three times per week.

https://doi.org/10.1016/j.heliyon.2018.e00982

Mice with eGFP expression under the proteolipid protein promoter were gifts from Jeff Rothstein, originally derived in the lab of Wendy Macklin (Mallon et al., 2002). Primary mouse Schwann cells were isolated in the same way as primary rat Schwann cells from the sciatic, median and ulnar nerves of P4 Plp-eGFP pups, except that the epineurium was not removed and no Ara-C or anti-Thy1 treatment was performed. Transgene expression was confirmed in biopsies by epifluorescent microscopy prior to cell isolation, and only positive pups used. Nerves from the positive pups of one litter were pooled prior to digestion. The percent GFP^+ cells, as determined by confocal microscopy, was similar between the two litters used for the *in vivo* studies (Fig. 2H).

Sensory neurons were isolated from Sprague Dawley rat day 14.5 embryo dorsal root ganglia (DRG). After dissection of the DRGs, they were transferred into L-15 media to which 100 μl of 10 mg/ml collagenase type I, 40 μl of 0.25% Trypsin-EDTA, and 15 μl of 25 mg/ml DNase was added. The tissue was incubated at 37 °C for 45 min, washed twice and then plated onto 12 mm PDL/laminin-coated glass slides (Thermo Fisher) at 30 000 cells in a 100 μl droplet of Neurobasal media supplemented with 1x B27 supplement, 1x Glutamax (Thermo Fisher), 50 ng/ml NGF (Alomone Labs, Jerusalem, Israel), and 10 μg/ml of piperacillin and ciprofloxacin (Sigma-Aldrich). After 1.5 hours, media was added to fill the well. Cells were purified the next day by adding 10 μM of both uridine and 5-fluoro-2′-deoxyuridine (FuDR, Sigma-Aldrich) for 2−3 days, kept 2 days in regular culture media, followed by another 2 day purification treatment. After this, mitotic cells could no more be observed in the cultures. Media was exchanged three times per week, and the cells underwent at least two media changes after completing the purification before initiating co-culture experiments.

2.3. Schwann cell and DRG neuron co-cultures

6 well plates of tissue culture polystyrene were coated with collagen (Nutragen, 1:30 dilution, Advanced BioMatrix), and purified rat Schwann cells at passage 4−6 after isolation were seeded at 100 000 cells/well. The following day, 8 μg/ml of polybrene (Sigma-Aldrich) was added to the media together with the lentiviral vectors used for the respective assay (see below). The next day, the media was removed, cells washed two times with PBS, and then detached using Accutase. The cells from one transduced well were seeded onto four cover slips with purified DRG neurons in media composed of EMEM (Quality Biological), 4 mg/ml D-glucose (Sigma-Aldrich), 50 ng/ml NGF, and 1% HI-FBS. After three days of co-culture, half the media volume was replaces and ascorbic acid supplemented to a final concentration of 50 μg/ml to induce myelination. Approximately half the media was replaced daily throughout the time of the co-culture, adjusting for some evaporation, with the ascorbic acid prepared fresh every time from powder. This was done not to expose the cells directly to the ambient air, but to keep them constantly hydrated.

https://doi.org/10.1016/j.heliyon.2018.e00982

For comparing the effects of the different transcription factors, the cells received the vectors at an MOI of 5 for each vector used, except for *Sox10*, which was given at an MOI of 1.17 due to poor viral titers. Groups included nuclear *Gfp* vector alone, or the nuclear *Gfp* vector plus one or all of the transcription factors as pooled viral solutions. Samples were collected at three weeks after the first ascorbic acid addition.

To further investigate the effects of *Egr2*, cells were treated as above with lentiviruses encoding nuclear *Gfp* or *Egr2-Myc-DDK* (*i.e.* not combining the vectors) at an MOI of 1, and compared to naïve, non-transduced cells. Samples were collected at three weeks after the first addition of ascorbic acid. *Egr2*-transduced cells were identified by the presence of the *Myc* epitope tag. This treatment was also used for the EdU and TUNEL assays, but at shorter time points (see below).

2.4. EdU incorporation assay

Schwann cell and DRG co-cultures were pulse-labeled by replacing half the media volume with fresh media containing 20 μM 5-ethynyl-2-deoxyuridine during the first and second media change at which ascorbic acid was also added. This was only done to samples used for proliferation assays; Schwann cells transduced with the *Egr2-Myc-DDK* vector, *nuclear-GFP,* and naïve cells. Two days after the first addition, cells were fixed using 4% paraformaldehyde in PBS for 10 minutes at room temperature, and stored in PBS at 4 °C until staining. The cells were then labeled using the Click-iT® 555-EdU assay (Thermo Fisher), before staining for S100β with an AlexaFluor 647 secondary as described below. Four samples per group were used, imaging two regions per sample and counting only S100β-labeled cells to specifically detect Schwann cells. Samples were also stained with the anti-Myc antibody with an AlexaFluor 488 secondary, but the anti-Myc had gone bad and this channel was excluded from the analysis.

2.5. TUNEL assay

Schwann cell and DRG co-cultures, for Schwann cells transduced with the *Egr2-Myc-DDK* vector, *nuclear-GFP,* and naïve cells, as well as controls containing only DRG cells, were fixed with 4% paraformaldehyde in PBS for 10 min at room temperature, before immediately staining with the ApopTag Red kit (Millipore) according to the manufacturer's instructions. Negative control samples using isolated DRG cells were prepared by omitting the TdT enzyme step. After this stain, the samples were stained as described for the EdU assay, again not using the anti-Myc stain in the analysis.

2.6. Immunocytochemistry

At the completion of the assays, samples were fixed with 4% paraformaldehyde in PBS for 10 min at room temperature, and either directly processed or stored at

https://doi.org/10.1016/j.heliyon.2018.e00982

4 °C in PBS until staining. Samples were then permeabilized using 0.3% Triton X-100 (Sigma-Aldrich) in PBS for 20 min at room temperature, rinsed three times with PBS, and then blocked for one hour in PBS containing 5% normal goat serum (Sigma-Aldrich). Primary antibody incubations were carried out over night at 4 °C in the blocking buffer, with antibody dilutions according to Table 1. Samples were then washed five times over 25 min with PBS, and incubated with secondary antibodies for one hour at room temperature. Apart from a Cy3-conjugated goat anti-mouse IgG2b antibody (Jackson Immuno Research Laboratories Inc., West Grove, PA, USA) used at a 1:200 dilution, all other secondaries were AlexaFluor conjugated and raised in goat used at a 1:500 dilution (Thermo Fisher) in blocking buffer. The incubation was followed by five washes over 25 min with PBS, and samples were then mounted using ProLong Diamond Anti-Fade with DAPI (Thermo Fisher). Imaging was performed using a Zeiss LSM 780 system, and images presented are maximum intensity projections from confocal Z-stacks.

Myelination frequencies were quantified by marking nuclei that expressed the reporter (Myc or nuclear GFP) in images of its channel, then separately marking nuclei associated with myelin segments in images from the MBP channel. These markings were then overlaid and double-labeled nuclei over total reporter gene nuclei was calculated to give the frequency of myelination.

2.7. Nerve guide preparation and engraftment

Mouse cells isolated from *Plp-eGFP* mouse pups (see above) were cultured for two days after isolation, with or without transduction using the bi-cistronic expression vector for *Egr2* and *mCherry* at MOI = 1, before dead cells were washed off using PBS, the remaining cells detached using Accutase, and resuspended in a solution of 16 mg/ml of fibrinogen in PBS at 10 million cells/ml, and combined at a 1-to-1 volumetric ratio with a 0.2 U/ml thrombin solution in PBS. For each nerve guide, 2.3 μl of the solution was loaded into a silicon tube (Dow Corning, Midland, MI, USA,

Table 1. Antibodies used for immunostaining assays.

Antigen	Vendor	Catalog number	Dilution or Concentration	Host species and isotype
Myelin basic protein	BioLegend	808401	1:1000	Mouse IgG2b
Neurofilament H	Millipore	AB1989	1:400	Rabbit IgG
S100β	DAKO	Z0311	1:400	Rabbit IgG
c-Myc	DSHB	AB_2266850	1:200 from concentrate	Mouse IgG1κ
p75 NGF receptor	Sigma-Aldrich	N3908	1:1000	Rabbit IgG
Glial fibrillary acidic protein	DAKO	Z0334	1:500	Rabbit IgG
β (III) tubulin	Synaptic systems	302304	1:1000	Guinea Pig IgG

https://doi.org/10.1016/j.heliyon.2018.e00982

inner diameter = 0.76 mm, outer diameter = 1.65 mm) and allowed to gel before cutting the tube 1 mm from each end of the gel. This created nerve guides with a 5 mm gel and 1 mm empty tubing at the ends, with a total length of 7 mm. Nerve guides without cells were created in the same way but omitting cells from the solution.

All animal procedures were carried out in accordance with and under protocols approved by the Johns Hopkins University IACUC. Adult (29−36 g, 4−6 months old) male NOD.CB17-Prkdc$^{scid/}$SzJ mice were anesthetized under inhalation anesthesia of 1−3% isoflurane using VetEquip system. The sciatic nerve was exposed and a 2 mm segment removed at the mid-thigh level. Proximal and distal ends were inserted into the 1 mm empty segment of the nerve guide, secured using 10-0 sutures to create a 5 mm gel-filled gap between the ends within the nerve guide. Wounds were closed using surgical clips. None of the experimental animals displayed any signs of autotomy over the period of the studies.

2.8. Immunohistochemistry

One month post-engraftment, animals were sacrificed and tissue collected and fixed in 4% PFA in PBS at 4 °C for 4−7 hours. The samples were then incubated in increasing sucrose concentrations, 15% and 30%, each for 2−4 days, before embedding in Tissue-Tek O.C.T. (Electron Microscopy Sciences, Hatfield, PA, USA) and sectioning to 20 μm sections using a cryostat onto Superfrost Plus microscope slides (Thermo Fischer). Control samples were prepared from contralateral control nerves.

Sections were permeabilized with 0.3% Triton X-100 (Sigma-Aldrich) in PBS for 20 min at room temperature, and then washed twice for two minutes with PBS. Blocking was performed using the M.O.M. Mouse IgG Blocking Reagent (Vector Laboratories, Burlingame, CA, USA) for one hour at room temperature. Samples were then rinsed twice with PBS for two minutes each, before incubating for 5 minutes with M.O.M. diluent at room temperature. Primary antibodies were diluted in the same solution according to Table 1, and incubated at 4 °C over night. The following day, the samples were washed five times over 25 min with PBS before incubating with secondary AlexaFluor-conjugated antibodies (Thermo Fisher) at 1:500 dilution for one hour at room temperature. Washing was performed five times with PBS over 25 min, before mounting with ProLong Diamond anti-fade with DAPI (Thermo Fisher). Positive controls as well as negative controls where primary antibodies were omitted to account for non-specific binding were performed on contralateral control nerve tissue samples, and images acquired using a Zeiss LSM 780 scanning laser confocal microscope system (Carl Zeiss Microscopy GmbH, Jena, Germany).

Engrafted Schwann cells, identified by the Plp-eGFP expression, were analyzed in transverse cross-sections at the mid-graft level in cells with their nuclei visible in

https://doi.org/10.1016/j.heliyon.2018.e00982

the cross-section. Adjacent sections were not used to avoid double counting cells, and myelination was identified by the nucleus associated with an MBP^+ ensheathing structure.

2.9. Statistical analysis

Statistical analysis was carried out using R (R Core Team, 2015), and GraphPad Prism (GraphPad Software). Effects of the different transcription factors were compared to the *Gfp* only control group (Fig. 1A) using the Dunnett's multiple comparison test. Direct comparisons of myelination frequency, EdU incorporation and TUNEL assays between groups were performed using Fisher's exact test, and 95% confidence intervals for the individual means, as depicted in the graphs, were computed using a binomial test. Myelination frequency and number of GFP^+ cells in tissue samples were compared using Student's t-test, and axon count and cross-section area of tissue samples were compared using ANOVA followed by Tukey's post hoc test. Results were considered statistically significant at $p < 0.05$.

3. Results and discussion

To test if overexpression of *Sox10, Oct6, Brn2 and/*or *Egr2* could potentiate myelination, we isolated and purified primary rat Schwann cells from postnatal day 5 pup sciatic nerves, transduced them with a nuclear GFP lentiviral vector plus vectors for one or all of the four factors, and seeded them onto purified sensory neurons isolated from embryonic day 14.5 rat dorsal root ganglia. Compared with cells transduced with the nuclear GFP vector alone, cells co-transduced with *Egr2* yielded 10 times more myelin segments per sample in the co-culture. None of the other combinations showed an increased number of myelin segments per sample (Fig. 1A and B). Closer examination however showed a relatively poor overlap of GFP^+ cells with the myelin segments (Fig. 1B). This could be due to poor co-transduction, but could also indicate that viral transduction itself is detrimental to myelination, and that the effects were not directly related to the overexpression of *Egr2*. We therefore used cells transduced with lentiviruses carrying *Egr2* with C-terminal epitope tags (*Egr2-Myc-DDK*). This allowed us to directly analyze the myelination frequency in cells overexpressing the *Egr2* transgene by staining for the Myc epitope tag. *Egr2*-overexpressing cells myelinated at a threefold higher frequency than naïve, non-transduced cells (Fig. 1C). Also, transduction with nuclear GFP had no observable effect over naïve cells (Fig. 1G–I), indicating that the effect was from *Egr2* overexpression and not an artifact from lentiviral transduction or from contaminating glia in the DRG isolations. An EdU assay carried out two days after myelination had been induced by the addition of ascorbic acid (five days total into the co-culture period) showed a decreased mitotic activity in the *Egr2*-transduced cells (Fig. 1D and E), in line with previous *in vivo* reports (Topilko et al., 1994; Zorick et al.,

https://doi.org/10.1016/j.heliyon.2018.e00982

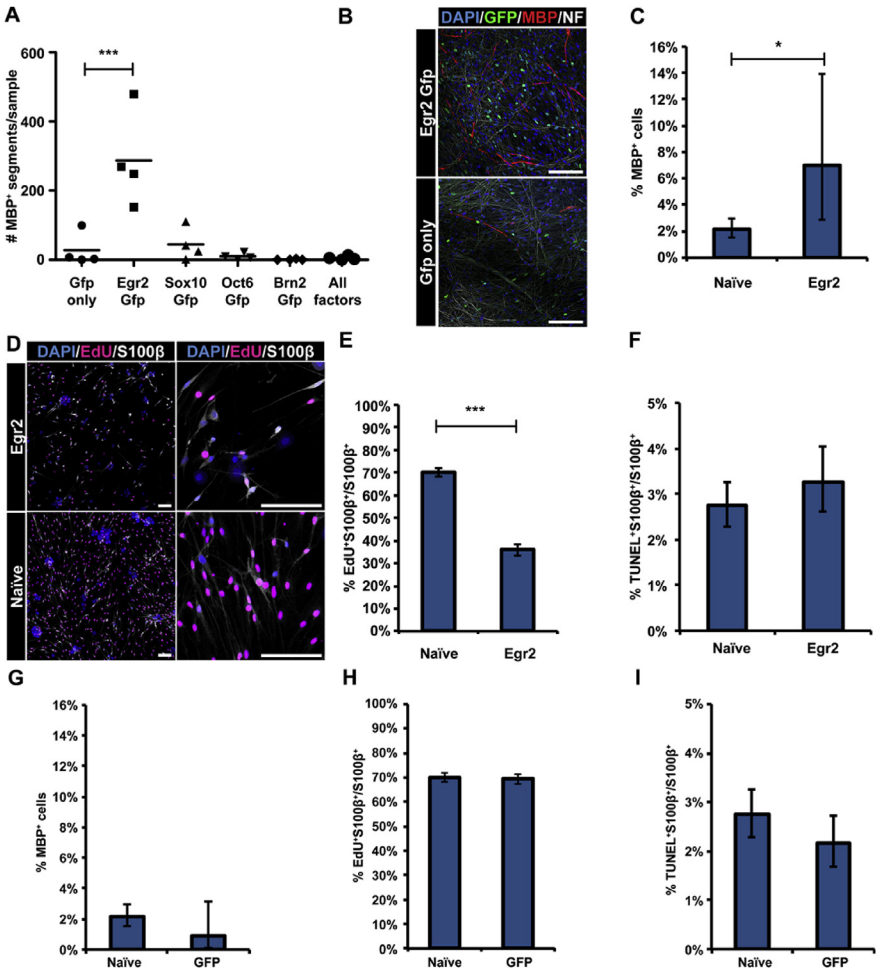

Fig. 1. Enhanced myelination frequency through *Egr2* transduction of rat Schwann cells in co-culture with rat DRG neurons. (A−B) Increased number of myelin segments detected in *Egr2*-transduced group compared to *Gfp* only transduction, but not for the other factors *Sox10*, *Oct6* or *Brn2,* as determined from tile scans of whole cover slips. (C) Cells transduced with *Egr2-Myc-DDK* vector showed an increased myelination frequency compared to naïve, non-transduced cells. (D−E) Reduced proliferation seen by EdU assay over the first two days after addition of ascorbic acid to the co-culture seen in *Egr2*-transduced Schwann cells ($S100\beta^+$ fraction). (F) No significant difference in cell apoptosis between *Egr2*-transduced and naïve Schwann cells detected through TUNEL assay at day 2 after addition of ascorbic acid to co-cultures ($S100\beta^+$ fraction). (G−I) Transduction with a nuclear GFP vector had no significant effects on (G) myelination frequency, (H) proliferation, or (I) apoptosis compared to naïve cells. Scale bars = 100 μm. $*p < 0.05$. $***p < 0.0001$. Error bars = 95% CI.

1999). This also confirmed that the enhanced myelination was indeed a true functionalization, and not a positive selection of the transduced cells, which would have instead been related to an increase in proliferation of *Egr2*-transduced cells. Only limited cell death was observed for all groups over the period of the co-culture, and a TUNEL assay carried out two days after myelination induction in the co-cultures confirmed very low and comparable levels of cell death between naïve and *Egr2*-transduced cells (Fig. 1F). Thus, these results show that

https://doi.org/10.1016/j.heliyon.2018.e00982

overexpression of *Egr2* can enhance the *in vitro* myelination frequency of primary rat Schwann cells.

Next we tested whether or not these effects would also be manifested *in vivo*. We isolated cells from the sciatic, median and ulnar nerves of postnatal day 4 transgenic mice in which eGFP was expressed under the control of the proteolipid protein promoter (Plp-eGFP mice), resulting in Schwann cells being GFP-positive within peripheral nerve tissue (Fig. 2G). In order to assess the effect of *Egr2* overexpression, we utilized a 5-mm sciatic nerve gap model supported by a silicone tube filled with a fibrin hydrogel, a model system commonly used in experimental studies of nerve repair (Lichtenfels M et al., 2013). The silicone tube could easily

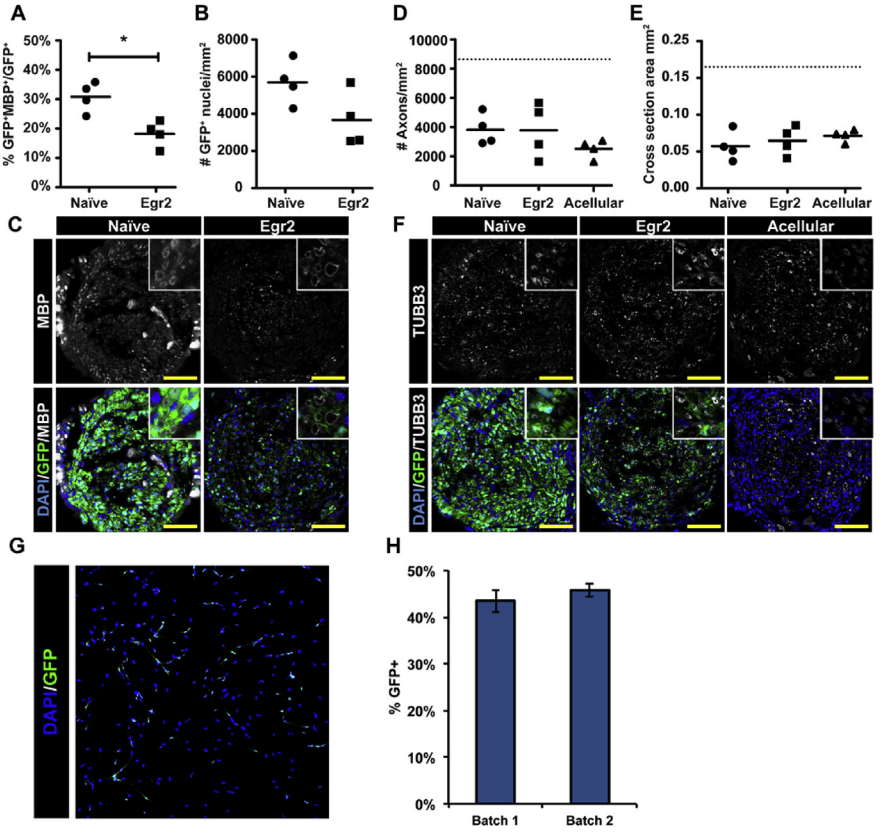

Fig. 2. *Egr2* overexpression reduces the myelination frequency in a mouse sciatic nerve engraftment model, analyzed at one month post engraftment. (A) Frequency of myelination, reported as percentage of graft-derived (GFP^+) cells that are associated with MBP^+ segments. (B) Density of graft-derived cells. (C) Representative images of anti-MBP staining. Inserts show images at a higher magnification. (D) Axon density determined by staining against β-(III)-tubulin (Tubb3), with dashed line indicating the level found in a contralateral control nerve. (E) Tissue cross-section area after removal of the supporting silicon tube, with dashed line indicating the level found in a contralateral control nerve. (F) Representative images of anti-Tubb3 staining. Inserts show images at a higher magnification. All samples were analyzed in transverse cross-sections at the mid-graft level, with n = 4 animals per group. Scale bars = 50 μm. *$p < 0.05$. (G–H) Percent GFP^+ cells was comparable between the two litters used for *in vivo* experiments one day after isolation from Plp-eGFP mice.

https://doi.org/10.1016/j.heliyon.2018.e00982

be sutured and was elastic to avoid nicking which would have been detrimental to the nerve regeneration. The fibrin gel was chosen due to controllable gelation properties and biodegradability, retaining the cells at the implantation site. The setup supported axonal growth and had suitable gelation times for cell seeding in preliminary experiments. Space restrictions at the site of engraftment in animals of this size only allowed for a gap length of 5 mm. Cells transduced with lentiviruses carrying an *Egr2* expression vector were seeded within fibrin hydrogels into silicon nerve guides bridging a 5 mm sciatic nerve gap in non-obese diabetic (NOD)-severe combined immunodeficiency (SCID) mice, and compared with animals receiving nerve guides with non-transduced cells or nerve guides with fibrin gel only, one month after engraftment. This mouse strain was chosen as it allowed for cell engraftment without the requirement for daily injections with immunosuppressive agents, *e.g.* cyclosporine, which would have been required in immune competent mice and its efficacy would have added another factor of variation between individual mice. A study in our lab found axonal regeneration and myelin debris clearance to be comparable between three different mouse strains with deficiencies in the adaptive immune system to that of wild type mice (Cashman and Höke 2017). Naïve cells were used as the control as our *in* vitro results did not show a significant effect on myelination frequency, proliferation, or apoptosis between naïve and non-transduced cells (Fig. 1G−I). Contrary to the previous *in vitro* results, the engrafted cells from the non-transduced group myelinated at a higher frequency than the cells from the *Egr2* overexpressing group (30.8% and 18.2% average myelination frequency respectively, $p < 0.05$, Fig. 2A).

As the frequency was analyzed in GFP^+ cells, *i.e.* normalized to the total number of visible graft-derived cells at the end-point, differences in proliferation were accounted for when calculating the relative frequencies. The cause for the difference between our *in vivo* and *in vitro* results are unclear, but could result from both the microenvironment in the *in vivo* model as well as from Schwann cell-intrinsic effects. Neuregulin 1 type I and III are key regulators of remyelination, and are expressed, respectively, by Schwann cells (Stassart et al., 2012) and by axons (Taveggia et al., 2005). Therefore, both the density of Schwann cells and axons can have an impact on the nerve regeneration microenvironment. We analyzed the axon density and number of graft-derived Schwann cells in transverse cross-sections at the mid-graft level. In line with our *in vitro* results, there was a trend for a lower average number of engrafted Schwann cells (GFP^+) in the *Egr2* overexpressing group, but this was not found to be statistically significant (Fig. 2B, $p = 0.0849$). In addition, the axon densities were similar between the groups receiving naïve and *Egr2*-transduced Schwann cells (Fig. 2D). While Schwann cell and axon densities can affect the levels of Neuregulin 1, enforced *Egr2* expression in Schwann cells does not affect their responsiveness to Neuregulin signaling (Parkinson et al., 2004). Additionally, Schwann cells grown in monoculture have

https://doi.org/10.1016/j.heliyon.2018.e00982

been reported to upregulate myelin gene expression in response to cAMP more readily when grown at low density (Monje et al., 2009). It is also worth noting that this experiment cannot confirm whether or not there was a difference in the time of axon ingrowth. While our *in vitro* results showed a higher myelination frequency when the cells were seeded onto a pre-established bed of axons, axon growth into the nerve guide occurs gradually over an extended period of time and may be impacted by the level of trophic support. Differences in axon growth rate could for instance arise from lowered trophic support from *Egr2*-transduced cells or simply differences in the number of supportive cells as discussed above. The timing of axonal contact could also impact myelin maturation, as later axonal contact would allow for less time to form mature myelin. On the other hand, the cross-section areas of the regenerating tissue were similar among all three groups (Fig. 2E), indicating that the amount of regenerated tissue was similar between the groups at the endpoint. The time from transduction to association with the axons is another possible explanation, and is also affected by the axon growth rate. *Egr2* expression has been found to have an inverse relation to the key repair Schwann cell regulator *cJun* (Arthur-Farraj et al., 2012; Parkinson et al., 2004), and a compromised ability to undertake this phenotype could affect their overall repair function, potentially playing a bigger role in the context of a full nerve repair model compared to the *in vitro* myelination assay. It is also possible that the level of *Egr2* expression in the transplanted cells is not optimized to increase the level of myelination, or that species differences play a role in the outcomes. The *in vitro* experiments were carried out using rat cells as these are more commonly employed with more robust culture methods than mouse cells, while the *in vivo* model used mice due to the availability of transgenic reporter lines that allowed us to track the engrafted Schwann cell population from non-purified cultures through the eGFP expression under the control of the Plp promoter.

In conclusion, this is the first report that *Egr2* overexpression can serve not only to up-regulate myelin transcripts, but to potentiate myelination *in vitro*. This effect did not, however, improve remyelination in the *in vivo* nerve repair model we employed, where cells were engrafted using a nerve guide containing a fibrin gel. Future studies are needed to address the cause of this discrepancy in order to harness a possible therapeutic effect from Schwann cell functionalization.

Declarations

Author contribution statement

Markus Tammia: Conceived and designed the experiments; Performed the experiments; Analyzed and interpreted the data; Contributed reagents, materials, analysis tools or data; Wrote the paper.

https://doi.org/10.1016/j.heliyon.2018.e00982

Ruifa Mi: Conceived and designed the experiments; Performed the experiments; Analyzed and interpreted the data.

Valentin Sluch, Allen Zhu, Tiffany Chung, Daniel Shinn, Don J. Zack: Contributed reagents, materials, analysis tools or data.

Ahmet Höke, Hai-Quan Mao: Conceived and designed the experiments; Analyzed and interpreted the data; Wrote the paper.

Funding statement

This work was supported by U.S. Department of Defense grant W81XWH-11-2-0047 and by a grant from The Dr. Miriam and Sheldon G. Adelson Medical Research Foundation. Markus Tammia acknowledges fellowship support from Stiftelsen Olle Engkvist Byggmästare, The Foundation Blanceflor Boncompagni Ludovisi née Bildt, and the Hans Werthén Foundation.

Competing interest statement

The authors declare no conflict of interest.

Additional information

No additional information is available for this paper.

Acknowledgements

The authors would like to thank Didier Trono and Eric Campeau for providing plasmids, and Dr. Jeffrey Rothstein for providing the Plp-eGFP mice.

References

Arthur-Farraj, P.J., et al., 2012. c-Jun reprograms Schwann cells of injured nerves to generate a repair cell essential for regeneration. Neuron 75, 633−647.

Bremer, M., et al., 2011. Sox10 is required for Schwann-cell homeostasis and myelin maintenance in the adult peripheral nerve. Glia 59, 1022−1032.

Brockes, J.P., et al., 1979. Studies on cultured rat Schwann cells. I. Establishment of purified populations from cultures of peripheral nerve. Brain Res. 165, 105−118.

Cashman, Höke, 2017. Deficiency of adaptive immunity does not interfere with Wallerian degeneration. PLoS One 12, e0177070.

Decker, L., et al., 2006. Peripheral myelin maintenance is a dynamic process requiring constant Krox20 expression. J. Neurosci. 26, 9771−9779.

 https://doi.org/10.1016/j.heliyon.2018.e00982

Ghislain, J., Charnay, P., 2006. Control of myelination in schwann cells: a Krox20 cis-regulatory element integrates Oct6, Brn2 and Sox10 activities. EMBO Rep. 7, 52–58.

Jaegle, M., et al., 2003. The POU proteins Brn-2 and Oct-6 share important functions in Schwann cell development. Genes Dev. 17, 1380–1391.

Jagalur, N.B., et al., 2011. Functional dissection of the Oct6 Schwann cell enhancer reveals an essential role for dimeric Sox10 binding. J. Neurosci. 31, 8585–8594.

Jessen, K.R., Mirsky, R., 2016. The repair Schwann cell and its function in regenerating nerves. J. Physiol. 594, 3521–3531.

Keilhoff, G., et al., 2006. Transdifferentiated mesenchymal stem cells as alternative therapy in supporting nerve regeneration and myelination. Cell. Mol. Neurobiol. 26, 1233–1250.

Latasa, M.-J., et al., 2010. Retinoic acid regulates myelin formation in the peripheral nervous system. Glia 58, 1451–1464.

Lichtenfels, M., et al., 2013. Effect of platelet rich plasma and platelet rich fibrin on sciatic nerve regeneration in a rat model. Microsurgery 33, 383–390.

Liu, Q., et al., 2012. Human neural crest stem cells derived from human ESCs and induced pluripotent stem cells: induction, maintenance, and differentiation into functional Schwann cells. Stem Cells Transl. Med. 1, 266–278.

Mallon, B.S., et al., 2002. Proteolipid promoter activity distinguishes two populations of NG2-positive cells throughout neonatal cortical development. J. Neurosci. 22, 876–885.

Monje, P.V., et al., 2009. Non-antagonistic relationship between mitogenic factors and cAMP in adult Schwann cell re-differentiation. Glia 57, 947–961.

Monuki, E.S., et al., 1990. Expression and activity of the POU transcription factor SCIP. Science 249, 1300–1303.

Nagarajan, R., et al., 2001. EGR2 mutations in inherited neuropathies dominant-negatively inhibit myelin gene expression. Neuron 30, 355–368.

Parkinson, D.B., et al., 2004. Krox-20 inhibits Jun-NH2-terminal kinase/c-Jun to control Schwann cell proliferation and death. J. Cell Biol. 164, 385–394.

R Core Team, 2015. R: A Language and Environment for Statistical Computing. R Foundation for Statistical Computing, Vienna, Austria. https://www.R-project.org/Last. (Accessed 13 May 2018).

Stassart, R.M., et al., 2012. A role for Schwann cell–derived neuregulin-1 in remyelination. Nat. Neurosci. 16, 48–54.

https://doi.org/10.1016/j.heliyon.2018.e00982

Stolt, C.C., Wegner, M., 2016. Schwann cells and their transcriptional network: evolution of key regulators of peripheral myelination. Brain Res. 1641, 101−110.

Taveggia, C., et al., 2005. Neuregulin-1 type III determines the ensheathment fate of axons. Neuron 47, 681−694.

Thoma, E.C., et al., 2014. Chemical conversion of human fibroblasts into functional Schwann cells. Stem Cell Rep. 3, 539−547.

Topilko, P., et al., 1994. Krox-20 controls myelination in the peripheral nervous system. Nature 371, 796−799.

Zorick, T.S., et al., 1999. Krox-20 controls SCIP expression, cell cycle exit and susceptibility to apoptosis in developing myelinating Schwann cells. Development 126, 1397−1406.

https://doi.org/10.1016/j.heliyon.2018.e00982